

Sliding Mode Observation and Control for Semiactive Vehicle Suspensions

Ravindra K. Dixit¹ and Gregory D. Buckner²

¹Emmeskay Inc., Plymouth, MI 48187, USA, rkdixit@emmeskay.com

²Department of Mechanical and Aerospace Engineering, North Carolina State University, Raleigh, NC 27695, USA, greg_buckner@ncsu.edu

Keywords: robust, nonlinear, sliding mode observer, sliding mode controller, semiactive vehicle suspension, MR damper.

Abstract:

This paper investigates the application of robust, nonlinear observation and control strategies, namely sliding mode observation and control (SMOC), to semiactive vehicle suspensions using a model reference approach. The vehicle suspension models include realistic nonlinearities in the spring and magnetorheological (MR) damper elements, and the nonlinear reference models incorporate skyhook damping. Since full state measurement is difficult to achieve in practice, a sliding mode observer (SMO) that requires only suspension deflection as a measured input is developed. The performance and robustness of sliding mode control (SMC), SMO, and SMOC is demonstrated through comprehensive computer simulations and compared to popular alternatives. The results of these simulations reveal the benefits of sliding mode observation and control for improved ride quality, and should be directly transferable to commercial semiactive vehicle suspension implementations.

1 INTRODUCTION

Active vehicle suspension systems were introduced in the early 1970's to overcome the drawbacks of passive suspensions, namely the inherent tradeoff between ride quality and handling performance [1,2,5]. Despite their published benefits, these systems remain complex, bulky, and expensive and are not common options on production vehicles. Semiactive suspensions overcome many of these limitations, albeit with a reduction in achievable ride quality and handling performance [1,2], though some researchers have concluded that this reduction is quite small [12]. Semiactive suspensions can be considerably more cost effective, compact, and functionally simple as they require only a variable damper and a few sensors to achieve adequate performance.

The recent introduction of commercial magnetorheological (MR) fluid dampers has enabled high-bandwidth, low-power control of suspension damping forces with very few mechanical parts [13,17]. These semiactive components contain suspensions of micron-sized, magnetizable particles in an oil-based fluid. In the presence of magnetic fields, these fluid particles become aligned with the field, dramatically increasing the fluid viscosity and effective damping. Recently, Carrera has introduced MagneShocks™ [13] and Delphi Automotive Systems has introduced Magneride™, both using MR fluid technology to enable semi-active damping adjustments at frequencies up to 1000 Hz.

The performance of semiactive suspension systems relies heavily on real-time control strategies. Early research focused primarily on linear techniques, such as optimal control [15,18-20] and skyhook control [16,21-23]. However, vehicle suspensions contain dynamic nonlinearities associated with springs and dampers [4], sliding friction in joints [4,24], and suspension kinematics [25] which significantly affect ride quality and handling performance. Vehicle

suspensions are also subjected to parameter variations, like changes in damping and stiffness over extended time periods that adversely affect the robustness of many algorithms.

For these reasons, recent semiactive control research has focused more on nonlinear control techniques. Gordon and Best [26] extended previous nonlinear optimal designs to semiactive systems and incorporated dynamic parameter optimization. Hedrick and Sohn [16] linearized the vehicle dynamics about an equilibrium point and applied skyhook control to control a semiactive MacPherson strut suspension. Henry and Zeid [27] derived a sub-optimal nonlinear control law, but did not consider spring and damper nonlinearities. Considerable research effort has concentrated on fuzzy logic, neural networks, and artificial intelligence techniques [14,28,29,30]. The primary advantages of these systems is that complete knowledge of the model dynamics may not be required, and hence nonlinearities may be incorporated easily. The primary drawbacks of such methods lie in the ad-hoc nature of their tuning and the inability to address robustness factors.

Sliding Mode Control (SMC) is a highly effective nonlinear and robust control strategy. It is insensitive to unmodeled dynamics and parametric uncertainties and has been used effectively in fields like robotics, aerospace, and automotive systems [31]. Kim and Ro [32] developed SMC for a nonlinear active suspension system and compared it to a self-tuning controller. Results showed that SMC significantly improved robust tracking performance when vehicle parameters changed. Alleyne and Hedrick [33] used SMC for a nonlinear actuator in an active vehicle suspension system. Hedrick et al. [34] demonstrated the effectiveness of SMC for MR semiactive suspension systems using a model following approach.

This paper investigates the application of robust, nonlinear observation and control strategies, namely sliding mode observation and control (SMOC), to semiactive vehicle suspensions using a

model reference approach. The vehicle suspension model includes realistic nonlinearities in the spring and MR damper elements, and the reference models are nonlinear versions of skyhook damping model. Since full state measurement is difficult to achieve in practice, a sliding mode observer (SMO) that requires only suspension deflection as a measured input is developed. The performance and robustness of sliding mode control (SMC), SMO, and SMOC is demonstrated through comprehensive computer simulations. The results presented quantify tracking errors between the plant and a skyhook reference model as a measure of performance, as skyhook models exhibit desirable ride quality and handling performance in most cases.

2 SYSTEM MODELS

This section summarizes the linear and nonlinear models used to describe the vertical vehicle suspension dynamics.

2.1 Quarter-Vehicle Model

The linear quarter-vehicle model (Figure 1) used routinely in the analysis and design of vehicle suspension systems [1,2,15,16,20] can be modified to include realistic nonlinearities associated with kinematics, bump-stops, stiction and hardening springs.

Here x_s and x_u represent the sprung and unsprung mass absolute displacements, respectively, x_0 represents the road disturbance, k_s and k_t represent suspension and tire stiffness, respectively. The suspension damping coefficient is the manipulated variable of the control system, and is thus time varying $b(t)$.

The suspension nonlinearities considered in this research include stiction, spring hardening and bump stops. Stiction is associated with Coulomb friction between the piston and cylinder, and occurs whenever the relative sliding velocity is zero and the static friction coefficient is significantly greater than the dynamic friction coefficient (Figure 2) [37,38].

This model incorporates the static friction force D_s (defined only when the suspension's relative velocity is zero) and the dynamic friction force C_s (for all other velocities):

$$f_{st} = \begin{cases} f_a & v = 0, |f_a| < D_s \\ D_s \operatorname{sgn}(f_a) & v = 0, |f_a| \geq D_s \\ C_s \operatorname{sgn}(v) + b_0 v & \text{otherwise} \end{cases} \quad (1)$$

where f_{st} represents the stiction force and f_a is the force applied to the damper.

Spring hardening and bump stops were incorporated using the polynomial stiffness model (2) formulated by Kim and Ro [32] (obtained by curve fitting measured data from the 1992 Hyundai Elantra front suspension) :

$$f_s = k_{s1}(x_s - x_u) + k_{s2}(x_s - x_u)^2 + k_{s3}(x_s - x_u)^3 \quad (2)$$

The nonlinear state equations for the semiactive, quarter-vehicle model are:

$$\begin{aligned} m_s \ddot{x}_s &= -f_s - f_{st} - b(t)(\dot{x}_s - \dot{x}_u) \\ m_u \ddot{x}_u &= f_s + f_{st} + b(t)(\dot{x}_s - \dot{x}_u) - k_t(x_u - x_0) \end{aligned} \quad (3)$$

2.2 MR damper dynamics

Damping forces in MR components are controlled by manipulating flux-producing coil currents. This approach is represented in the block diagram of Figure 3. The desired damping coefficient $b_d(t)$ determined by the suspension control algorithm must be related to a coil control current, which depends on the nonlinear force-velocity characteristics of the MR damper. The damping relationships used in this research (Figure 4) are based on a generic composite of high performance MR dampers used for vibration isolation and automotive semiactive suspensions [23,40]. The stiction characteristics (Section 2.1) are lumped into this composite MR damper model. The steady-state damping coefficient $b_{ss}(t)$ is both bounded and proportional to the applied current $i(t)$:

$$\begin{aligned} b_0 \leq b_{ss}(t) \leq b_{max} \quad \text{for } 0 \leq i(t) \leq i_{max} \quad \text{and} \\ b_{ss}(t) = b_0 + \mu i(t) \end{aligned} \quad (4)$$

Here μ is a constant that linearly scales the damping resulting from the applied coil current $i(t)$. The steady-state current required to achieve the desired damping coefficient $b_d(t)$ is thus:

$$i(t) = \frac{b_d(t) - b_0}{\mu} \quad (5)$$

Although the response times of commercial MR fluids are relatively fast, phase lag is associated with the inductance of the control coils. The dynamic response of a typical MR shock absorber can be modeled as first-order, linear, with a time constant τ of 1-10 ms [17,23,39]:

$$b(s) = \frac{b_{ss}}{\tau s + 1} \quad (6)$$

The static friction force D_s is assumed equal to the dynamic friction force C_s [23,40] which is time-varying, bounded, and proportional to the applied current:

$$\begin{aligned} C_{s \min} &\leq C_s(t) \leq C_{s \max} \\ C_s(t) &= C_{s \min} + \psi i(t) \end{aligned} \tag{7}$$

3 CONTROLLER DEVELOPMENT

High-performance control of semiactive vehicle suspensions is complicated by nonlinearities and uncertainties in the system dynamics and by the need for accurate state information. For these reasons, practical implementations require nonlinear controllers and observers that are robust to uncertainties and disturbances. In this section, a robust sliding mode controller is developed for the nonlinear, semiactive vehicle suspension system (3). Ideally, this controller will be robust to parameter variations (so-called structured uncertainties) and unmodeled dynamics (unstructured uncertainties). The controller is developed using a model reference approach that emulates the performance of the well-known skyhook damping model [21,23,32,34].

Advanced control strategies like model reference sliding mode control require knowledge of the absolute sprung mass velocity and displacement, states that are not readily measurable. This fact is frequently overlooked in simulations, but cannot be ignored in vehicle implementations. In this research, a robust observer is developed to provide state estimation using only measured suspension deflection as an input.

3.1 Model Reference Control

Model reference control (MRC) is a strategy based on specifying the desired closed-loop performance through the selection of a stable reference model (Figure 5).

In MRC, the plant output y is made to track a reference model output y_r using feedback control u . Practical challenges to this approach are imposed by physical plant constraints [23,34], minimum phase plant requirements [47], and accurate knowledge of states and inputs that may not be measurable [32,44].

3.1.1 Skyhook Reference Models

An excellent reference model for semiactive vehicle suspension control can be derived from Karnopp's skyhook damping strategy [16,21-23]. An inertially grounded damper (the “skyhook” damper, b_{sky}) provides damping proportional to the absolute velocity of the sprung mass. A fourth-order realization of this reference model (which assumes road inputs are known) is shown in Figure 6. The nonlinear state equations for this reference model are:

$$\begin{aligned} m_s \ddot{x}_{sr} &= -f_s - b_s (\dot{x}_{sr} - \dot{x}_{ur}) - b_{sky} \dot{x}_{sr} \\ m_u \ddot{x}_{ur} &= f_s + b_s (\dot{x}_{sr} - \dot{x}_{ur}) - k_t (x_{ur} - x_0) \end{aligned} \quad (8)$$

Here f_{st} and f are the nonlinear stiction and hardening spring relations defined in (1) and (2).

Because these suspension nonlinearities significantly affect the achievable performance of semiactive suspensions, and because plant “followability” is an inherent requirement of MRC, this nonlinear skyhook model is a more suitable reference model than linear alternatives.

3.2 Sliding mode control

Sliding Mode Control (SMC) is a high-performance, robust control strategy for uncertain nonlinear systems. The control law consists of two components: a stabilizing equivalent control law u_{eq} and a performance term u_p . Model reference SMC is based upon the formulation of a “sliding surface” of tracking errors, such that perfect tracking is equivalent to remaining on this surface for all time. The performance term is discontinuous over the sliding surface, and governs the reachability and global asymptotic stability of the system. The reference tracking errors \mathbf{e} and sliding surface $s(\mathbf{e}, t)$ are defined:

$$\begin{aligned} \mathbf{e} &= \left[(x_r - x) \quad (\dot{x}_r - \dot{x}) \quad \dots \quad \left(\frac{d^{n-l} x_r}{dt^{n-l}} - \frac{d^{n-l} x}{dt^{n-l}} \right) \right] \\ s(\mathbf{e}, t) &= \dot{\mathbf{e}} + \lambda \mathbf{e} \end{aligned} \quad (9)$$

where λ is a positive design scalar and $x_r(t)$ and $x(t)$ represent the states of the reference model and the plant, respectively. A system remaining on such a sliding surface is said to be in “sliding mode” and has zero tracking error, as the unique solution to $s(\mathbf{e}, t) = 0$ is $\mathbf{e}(t) = 0$ [45]. This reduces a high-order tracking problem to a first-order regulator problem in s . For the specific case of tracking a skyhook reference model, the sliding surface can be defined:

$$\begin{aligned} \mathbf{e} &= [x_{sr}(t) - x_s(t)] \\ s(\mathbf{e}, t) &= \dot{\mathbf{e}} + \lambda \mathbf{e} \end{aligned} \quad (10)$$

where $x_{sr}(t)$ is the sprung mass vertical displacement of the skyhook reference model.

Constructing a control strategy so that the system is in sliding motion is accomplished by formulating a continuous feedback control law u_{eq} and adding to it a discontinuous performance term u_p :

$$u = u_{eq} + u_p \quad (11)$$

3.2.1 Equivalent Control law

The equivalent control law is derived from the nonlinear state equations (3) and the defined sliding surface (10). Neglecting the MR damper dynamics (6), the quarter-vehicle dynamics can be expressed:

$$\begin{aligned} \ddot{x}_s &= -\frac{f_s + f_{st}}{m_s} - \frac{b_0}{m_s}(\dot{x}_s - \dot{x}_u) - \frac{I}{m_s}(\dot{x}_s - \dot{x}_u)b(t) \\ &= f(x) + g(x)u \end{aligned} \quad (12)$$

where $u=b(t)$ is the desired damping coefficient determined by the controller, and:

$$\begin{aligned} f(x) &= -\frac{f_s + f_{st}}{m_s} - \frac{b_0}{m_s}(\dot{x}_s - \dot{x}_u) \\ g(x) &= -\frac{I}{m_s}(\dot{x}_s - \dot{x}_u) \end{aligned} \quad (13)$$

Since $f(x)$ and $g(x)$ are not known precisely (due to parametric uncertainties and unmodeled dynamics), SMC must assume that modeling uncertainties are bounded. The additive plant uncertainties can be bounded by a constant (or known function) $F = F(x, \dot{x})$ [45]:

$$|f(x) - \hat{f}(x)| \leq F \quad (14)$$

where $\hat{f}(x)$ and $\hat{g}(x)$ are uncertain models of $f(x)$ and $g(x)$. The multiplicative plant uncertainties can be bounded by known functions (or constants) $g_{min} = g_{min}(x, \dot{x})$ and $g_{max} = g_{max}(x, \dot{x})$ [45]:

$$0 < g_{\min} \leq \hat{g}(x) \leq g_{\max} \quad (15)$$

As shown in [45], it is advantageous to choose $\hat{g}(x)$ as the geometric mean of g_{\min} and g_{\max} :

$$\hat{g} = \sqrt{g_{\min} g_{\max}} \quad (16)$$

The equivalent control law is designed to maintain the system on the sliding surface in the absence of modeling uncertainties. If $f(x)$ and $g(x)$ were known perfectly, equivalent control would be enough to keep the system (12) on the sliding surface for all time ($s=0 \Rightarrow \dot{s}=0 \quad \forall t$). With modeling uncertainties, however, the sliding condition can be determined by combining (10) and (12):

$$\begin{aligned} \dot{s}(\mathbf{e}, t) &= \ddot{\mathbf{e}} + \lambda \dot{\mathbf{e}} \\ &= \ddot{x}_{sr} - \ddot{x}_s + \lambda \dot{\mathbf{e}} \\ &= \ddot{x}_{sr} - (\hat{f}(x) + \hat{g}(x)u) + \lambda \dot{\mathbf{e}} \end{aligned} \quad (17)$$

The equivalent control law is thus:

$$u_{eq} = \hat{g}(x)^{-1} (-\hat{f}(x) + \ddot{x}_{sr} + \lambda \dot{\mathbf{e}}) \quad (18)$$

3.2.2 Discontinuous performance term

Uncertainties in $f(x)$ and $g(x)$ may cause the system to leave sliding surface defined by (10).

To ensure robustness, a discontinuous performance term u_p (also known as a switching term) is introduced. When the system leaves the sliding surface (i.e. $s \neq 0$), this term drives the system states back onto the sliding surface by making it attractive:

$$u_p = -\hat{g}(x)^{-1} k \cdot \text{sgn}(s) \quad (19)$$

where sgn is the signum function defined by:

$$\begin{aligned} \text{sgn}(s) &= +1 \quad \text{if } s > 0 \\ \text{sgn}(s) &= -1 \quad \text{if } s < 0 \end{aligned} \quad (20)$$

The switching gain k is generally a constant determined by the uncertainty bounds (14), but it may be time- or state-dependent. In this research the switching gain is state-dependent, which allows for reduced control effort in areas where modeling uncertainties are small. The condition on k for robust stability is:

$$k \geq \alpha(F + \eta) + (\alpha - 1) |\hat{g}u_{eq}| \quad (21)$$

where $\alpha = \sqrt{g_{\max}/g_{\min}}$, F is defined in (14), and η is a strictly positive constant defined using the η -reachability condition [31,45]:

$$\frac{1}{2} \frac{d}{dt} s^2 \leq -\eta |s| \quad (22)$$

It can be shown [45] that with this choice of switching gain, global asymptotic stability is ensured.

Combining (11), (18), and (19) the SMC law is:

$$u = u_{eq} + u_p = \hat{g}^{-1} \left[\left(-\hat{f}(x) + \ddot{x}_{sr} + \lambda \dot{\mathbf{e}} \right) - k \text{sgn}(s) \right] \quad (23)$$

3.3 Sliding Mode Observation

The SMC law (23) derived above requires accurate knowledge of the absolute sprung mass displacement and velocity, since these variables are used to formulate the sliding surface. These measurements are not readily attainable on a moving vehicle, however, hence for this research a Sliding Mode Observer (SMO) was developed. SMOs enable robust, accurate estimation of system states for nonlinear, uncertain systems where conventional observers or Kalman filters perform poorly [8,27].

3.3.1 SMO Design

For purposes of state estimation, the nonlinear state equations (4) can be expressed in the following form:

$$\begin{aligned}\dot{x} &= Ax + Bv(x,t) + Gx_0 + Df(x,t) \\ y &= Cx\end{aligned}\tag{24}$$

where $x = [x_u \quad \dot{x}_u \quad x_s \quad \dot{x}_s]^T$ represents the state vector, $v(x,t) = b(t)(\dot{x}_u - \dot{x}_s)$ represents the controlled damping force, $f(x,t) = f_s + f_{st}$ represents suspension nonlinearities, x_0 represents exogenous road inputs, and y represents the measured output (suspension deflection). A and B are the system and input matrices, respectively. G and D scale the exogenous road inputs and nonlinear system terms, respectively. C is the output matrix.

The block diagram in Figure 7 shows the structure of a conventional observer, in this case applied to the nonlinear state equations (3). The actual plant output y is compared with the observed output, \hat{y} , and the error is used to update the observed states by means of the observer matrix L . For this nonlinear application, the separation principle [47] cannot be applied, thus closed loop

stability cannot be guaranteed. Given a nominal model of this plant, the nonlinear observer is represented by [41,42]:

$$\dot{\hat{x}} = A\hat{x} + Bv(\hat{x}, t) + Df(\hat{x}, t) + L(y - \hat{y}) \quad (25)$$

where:

- \hat{x} represents the estimated state vector $\begin{bmatrix} \hat{x}_u & \dot{\hat{x}}_u & \hat{x}_s & \dot{\hat{x}}_s \end{bmatrix}$
- y represents the actual plant output, in this case suspension deflection $x_s - x_u$
- \hat{y} represents the estimated plant output $\hat{x}_s - \hat{x}_u$
- L is the observer matrix

The L matrix can be designed [27] by placing the poles of the system matrix $[A-LC]$ to achieve stable error dynamics.

$$\begin{aligned} e_o &= y - \hat{y} \\ \dot{e}_o &= (A-LC)e_o + Df(e_o, t) + Gx_0 \end{aligned} \quad (26)$$

This traditional observer structure cannot guarantee global asymptotic stability, robustness, or convergence in the presence of plant nonlinearities, parametric variations, and disturbances. For this reason, a discontinuous performance term, similar to the SMC switching term in (19), is added for robustness:

$$\dot{\hat{x}} = A\hat{x} + Bv(\hat{x}, t) + Df(\hat{x}, t) + L(y - \hat{y}) + K_0 \text{sgn}(y - \hat{y}) \quad (27)$$

where K_0 is the SMO switching gain matrix. Typically K_0 is designed using LQ techniques [41,43] or Nyquist criteria approaches [27,43]. In this research, the ‘‘circle criterion’’ approach has been used, resulting in the selection of $K_0 = \rho G$, $\rho \geq 0$ [27]. To avoid chattering, the performance term

$K_0 \text{sgn}(y - \hat{y})$ can be constrained to be continuous as long as the system states lie within a boundary layer defined by error limits between the measured and estimated output states:

$$x_p = K_o \cdot \text{sat} \left[\frac{y - \hat{y}}{\phi} \right] \quad (28)$$

where ϕ is the boundary layer width. When the observer error exceeds this boundary layer width, the performance term becomes discontinuous. The saturation term is thus defined to be:

$$\text{sat} \left[\frac{y - \hat{y}}{\phi} \right] = \begin{cases} \frac{y - \hat{y}}{\phi} & \text{for } |y - \hat{y}| \leq \phi \\ \text{sgn}(y - \hat{y}) & \text{for } |y - \hat{y}| > \phi \end{cases} \quad (29)$$

Combining (25) and (28) results in the complete SMO law:

$$\begin{aligned} \dot{\hat{x}} &= A\hat{x} + Bv(\hat{x}, t) + Df(\hat{x}, t) + L(y - \hat{y}) + K_o \text{sat} \left[\frac{y - \hat{y}}{\phi} \right] \\ \hat{y} &= C\hat{x} \end{aligned} \quad (30)$$

The structure of this robust observer is illustrated in Figure 8.

4 SIMULATIONS

Extensive computer simulations were conducted to evaluate the effectiveness of sliding mode observation and control for semiactive vehicle suspensions. These simulations utilized vehicle parameters and road input data from other authors to facilitate direct performance comparisons. Performance was quantified based on direct comparisons of sprung mass motion with respect to the skyhook reference model. These simulations are divided into different sets, each with separate

objectives, as summarized in Table 1. The following sections detail these computer simulation sets.

4.1 Vehicle and road parameters

The vehicle suspension parameters were assumed to be those of a 1992 Hyundai Elantra, as outlined in Ro and Kim [32] (Table 2).

Road input data was also taken from the literature to facilitate performance comparisons. Specifically, the harmonic inputs, filtered white noise, and actual road measurements found in Hać et. al. were implemented for simulations [18,46].

4.2 Controller parameters

The SMC law (23) utilizes a controller gain k that can be constant or state dependent. In either case, its magnitude is based on assumed uncertainty bounds between the model and actual vehicle. For these simulations, the additive plant uncertainties $(f - \hat{f})$ were assumed to be bounded within 30%:

$$F = 0.3\hat{f} = 0.3 \left[-\frac{f_s + F_{st}}{m_s} - \frac{b_0}{m_s} (\dot{x}_s - \dot{x}_u) \right] \quad (31)$$

Similarly, multiplicative uncertainties associated with \hat{g} were assumed to be bounded within 30%:

$$\begin{aligned}
g_{\max} &= -\frac{1}{1.3m_s}(\dot{x}_s - \dot{x}_u) \\
g_{\min} &= -\frac{1}{0.7m_s}(\dot{x}_s - \dot{x}_u) \\
\alpha &= \sqrt{g_{\max}/g_{\min}}
\end{aligned} \tag{32}$$

SMC design parameters η and λ , defined in (17) and (22), were tuned for optimal performance over a wide range of road inputs:

$$\eta = 1 \quad ; \quad \lambda = 120 \tag{33}$$

4.3 Simulation Set I: Fixed-Gain vs. Variable-Gain SMC

To investigate the performance implications of variable-gain SMC, simulations were conducted using fixed and variable switching gains k in the performance term (19). Performance indices J_1 and J_2 are reflect tracking error between the plant and the skyhook reference model:

$$J_1 = \frac{\sqrt{\sum_{i=1}^N (y_{ref}(iT) - y(iT))^2}}{NT} \tag{34}$$

$$J_2 = \max_i |y_{ref}(iT) - y(iT)| \cdot 10^3 \tag{35}$$

Performance index J_3 is based on sprung mass acceleration and suspension displacement:

$$J_3 = \sum_{i=1}^N [\ddot{x}_s(iT)^2 + \rho(x_s(iT) - x_u(iT))^2] \cdot T \tag{36}$$

For these simulations, $\rho = 100,000$ was selected to appropriately weight each component of J_3 .

A fixed switching gain of $k = 10$ was selected based on the peak of variable-gain simulations for a variety of road inputs. Fixed-gain simulation results revealed adequate tracking performance, especially for road inputs that resulted in moderate to large suspension deflections. In these cases, the sprung mass response closely resembled that of the fourth-order, nonlinear skyhook reference model (8). For road inputs resulting in small suspension deflections, however, the tracking performance was noticeably reduced. Figure 9 shows the controlled sprung mass response to a low-amplitude, white noise road input, with comparisons to the skyhook reference model and passive suspension responses. Performance indices are summarized in Table 3, along with peak suspension travel and sprung mass acceleration data.

Next, variable-gain SMC was evaluated. The switching gain in (19) was assumed to be state dependent as described in (21):

$$k = \alpha(F + \eta) + (\alpha - 1)|\hat{g}u_{eq}|$$

Variable-gain simulation results for the same white noise road input reveal significantly improved tracking performance vs. fixed-gain results, as illustrated in Figure 10. This improvement is quantified by comparing performance indices J_1 and J_2 for each case (Table 3). These results are typical for low-amplitude, high-bandwidth road inputs (resulting in small suspension deflections, moderate sprung mass accelerations), and are related to the “adaptability” provided by state dependent switching gains. For larger-amplitude road inputs, the differences in performance were less significant. Table 3 also shows that peak suspension travel and sprung mass acceleration were improved with variable-gain SMC (vs. fixed-gain SMC), although performance index J_3 increased slightly. All three indices were higher than the model reference and passive response cases, though well within acceptable levels.

Figure 11 shows the variations in switching gain $k(t)$ and MR damper current $i(t)$ over the course of this variable-gain SMC simulation, resulting in an average switching gain of $k = 3.51$. The tracking performance was clearly superior to fixed-gain SMC ($k = 10$). Additionally, the specific power consumption (calculated by integrating current) was $24.6 \text{ mW}/\Omega$ (of MR damper coil resistance) less for variable-gain SMC than for fixed-gain SMC. Similar results were obtained for other road inputs. Figure (12) shows a magnitude spectrum (FFT) of the control current $i(t)$ for this simulation. This figure reveals that the required bandwidth of the MR damper is less than 100 Hz for this road input. Note that the MR damper time constant used in these simulations was 1.0 msec, providing more than adequate bandwidth.

These simulations clearly revealed the performance advantages of variable-gain SMC, hence this control structure was utilized for all subsequent simulations.

4.4 Simulation Set II: Sliding Mode Observation and Control (SMOC)

The sliding mode observer structure introduced in Section 3.3 is repeated here for convenience:

$$\begin{aligned} \dot{\hat{x}} &= A\hat{x} + Bv(\hat{x}, t) + Df(\hat{x}, t) + L(y - \hat{y}) + K_o \text{sat} \left[\frac{y - \hat{y}}{\phi} \right] \\ \hat{y} &= C\hat{x} \end{aligned} \quad (37)$$

The state matrices of this equation were specified to be consistent with previous simulations:

$$\begin{aligned}
A &= \begin{bmatrix} 0 & 1 & 0 & 0 \\ -(k_s + k_t)/m_u & -b_0/m_u & k_t/m_u & b_0/m_u \\ 0 & 0 & 0 & 1 \\ k_s/m_s & b_0/m_s & -k_s/m_s & -b_0/m_s \end{bmatrix} \\
B &= [0 \quad -1/m_u \quad 0 \quad 1/m_s]^T \\
C &= [1 \quad 0 \quad -1 \quad 0] \\
D &= [0 \quad 1/m_u \quad 0 \quad -1/m_s] \\
G &= [0 \quad k_t/m_u \quad 0 \quad 0]^T
\end{aligned}$$

The observer feedback matrix L was designed to place the tracking error poles (26) at $[-23.09 \pm 70.58i, -21.16 \pm 12.27i]$, resulting in $L = [40 \ 40 \ -40 \ -400]^T$. The switching gain matrix and boundary layer width were set to $K_o = G$, $\phi = 0.001$.

To evaluate the performance of SMO, simulations were conducted for a variety of road inputs. Figure 13 shows that SMO estimate of sprung mass displacement is nearly indistinguishable from the actual state for a sinusoidal road input. For comparison, this figure also shows the output of a nonlinear observer (without the performance switching term (28)), which is clearly inferior. To separate observer performance from controller performance in this simulation, the observed states were not used by the controller (full state measurement was assumed).

To quantify observer performance, two additional performance indices were specified based on the RMS and peak errors between actual outputs and observed outputs:

$$J_4 = \frac{\sqrt{\sum_{i=1}^N (x_s(iT) - \hat{x}_s(iT))^2}}{NT} \quad (38)$$

$$J_5 = \max_i |x_s(iT) - \hat{x}_s(iT)| \cdot 10^3 \quad (39)$$

For the simulations shown in Figure 13, these indices reveal that the SMO performance is far superior to the conventional (non-switching) observer (Table 4). Similar results were obtained for a variety of road inputs.

Simulated performance using combined sliding mode observation and control (SMOC, using estimated state information for the control law) was also very good. For continuously varying road inputs (sinusoids, white noise, etc.) SMOC provided excellent tracking, as illustrated in Figure 14. This performance is quantified using the performance indices J_1 and J_2 (Table 5), which reveal nearly indistinguishable performance between full-state, variable-gain SMC and SMOC. These results are typical for continuously-exciting road inputs (white noise, sinusoids, etc.). However, for sudden road inputs (bumps, steps, etc.) the suspension stiction frequently resulted in small (0-5 mm) steady-state tracking errors that were not eliminated by control. Table 5 also shows that peak suspension travel and sprung mass acceleration (and accordingly performance index J_3) were high for all cases (including the skyhook reference model), but were considerably improved with SMC and SMOC when compared to the passive response.

4.5 Simulation Set III: SMOC with Parametric Uncertainties

The preceding SMO and SMOC simulations did not include parametric uncertainties in the state equations. Although the variable switching gains were based on 30% bounds on additive and multiplicative plant uncertainties (14) and (15), these parameters remained at their nominal values. To investigate the effects of parametric uncertainties on observer performance and controller robustness, simulations were conducted using 10% and 25% variations in spring stiffness ($k_{s,i}$) and

sprung mass (m_s), respectively. These simulations revealed the benefits of the switching term (28), as observer performance was excellent, particularly for continuously varying road inputs (Figures 15 and 16).

Simulations were conducted to evaluate the performance implications of parametric uncertainties using combined sliding mode observation and control (SMOC). Figures 17 and 18 show the performance of SMOC for sinusoidal and white noise road inputs, respectively. The impact of parametric uncertainties can be evaluated by comparing Figure 17 to Figure 14 (without uncertainties). This comparison makes it clear that the SMOC is robust to these uncertainties, as the performance is similar. The performance to white noise inputs (Figure 18) is even better. As before, performance is quantified using the performance indices J_1 , J_2 , and J_3 (Tables 6 and 7), which reveal slight degradations from cases without uncertainties. Tables 6 and 7 also show that peak suspension travel and sprung mass accelerations were high for the sinusoidal road inputs, but were considerably improved with SMOC when compared to the passive response.

5 CONCLUSION

Semiactive vehicle suspensions contain nonlinearities and parametric uncertainties that require robust nonlinear control for peak performance. Additionally, the state information required for formulating a control law online is almost never available in practice. While these issues are frequently overlooked in simulations [14,15,18,20], they cannot be overlooked in real-time implementations.

In this research, the performance of sliding mode observation and control for semiactive vehicle suspensions was established through extensive computer simulations. These comprehensive

simulations investigated the effects of suspension nonlinearities, parametric uncertainties, and state estimation. Model reference SMC was implemented using a nonlinear skyhook reference model. Results showed that the suspension system was able to track the characteristics of the reference model with good accuracy. Simultaneously the bandwidth required by this control strategy was a fraction of the bandwidth available in a MR damper. A sliding mode observer was designed and implemented. It performed well for a variety of road inputs, even in the presence of parametric uncertainties. The performance and robustness of combined sliding mode observation and control (SMOC) was confirmed through extensive simulations. Performance benefits were more pronounced for large-amplitude, limited-bandwidth road inputs (sinusoids) than for low-amplitude, high-bandwidth inputs (white noise).

The results of this research should be directly transferable to actual semiactive vehicle suspension implementations. The effects of realistic nonlinearities, parametric uncertainties, unmeasurable states and road inputs have all been investigated through comprehensive simulations. The results of these simulations reveal the benefits of sliding mode observation and control for improved ride quality.

6 REFERENCES

- [1] Seung-Jin Heo and Kihong Park, "Performance and design considerations for continuously controlled semiactive suspension systems", *Int. J. of Vehicle Design*, vol. 23, no.3, pp. 376-389, 2000.
- [2] R. S. Sharp and S. A. Hassan, "Performance and design considerations for dissipative semiactive suspension systems for automobiles", *Proc. of the Instn. of Mech. Engrs.*, vol. 201, no. D2, pp. 149-153, 1987.

- [3] G. D. Buckner, K. T. Schuetze, and J. H. Beno, "Intelligent feedback linearization for active vehicle suspension control", *ASME J. of Dynamic Systems, Measurement, and Control*, vol. 123, no. 4, pp. 727-733, 2001.
- [4] G. D. Buckner, K. T. Schuetze and J. H. Beno, "Active vehicle suspension control using intelligent feedback linearization", *Proc. of the 2000 American Controls Conference*, vol. 6, pp. 4014-18, 2000.
- [5] R. S. Sharp and S. A. Hassan, "The relative performance capabilities of passive, active and semiactive car suspension systems", *Proc. of the Instn. of Mech. Engrs., Part D*, 1986, vol. 200 (D3), pp. 219-228.
- [6] A. G. Thompson, "Design of active suspensions", *Proc. of the Instn. of Mech. Engrs.*, vol. 185, no. 36, pp. 553-563, 1970.
- [7] D. A. Crolla, R. H. Pitcher and J. A. Lines, "Active suspension control for an off-road vehicle", *Proc. of the Instn. of Mech. Engrs., part D1*, vol. 201, pp. 1-10, 1987.
- [8] Rajesh Ramani and J. K. Hedrick, "Adaptive observers for active automotive suspensions: theory and experiment", *IEEE Transactions on Control Systems Technology*, vol. 3, no. 1, pp. 41-54, 1995.
- [9] P.G.Wright and D.A.Williams, "The application of active suspension to high performance road vehicles", *Microprocessors in Fluid Engineering*, IMechE conference publications, 1984.
- [10] S.T. Hung, I. Kanellakopoulos, V. Kokotovic, and P. V. Kokotovic, "Active suspension studies: modeling, identification and analysis", *Ford Motor Company Report AS-88-2*, September 1988.
- [11] Scott Memmer, "Suspension III: active suspension systems", *Edmunds Technical Center Articles*, <http://www.edmunds.com/ownership/techcenter/articles/43853/article.html>, April 2001.
- [12] D. Karnopp, "Theoretical limitations in active suspensions", *Vehicle System Dynamics*, vol. 15, pp. 41-54, 1986.
- [13] Magneshock, "2nd generation magneshock", *Carrera Racing Shocks Quarterly News*, http://www.carrerashocks.com/Newsletter_spring_2001_P2.htm, 2001.
- [14] C. F. Nicolas, J. Landaluze, E. Castrillo, M. Gaston, and R. Reyero, "Application of fuzzy logic control to the design of semiactive suspension systems", *IEEE International Conference on Fuzzy System*, vol. 2, pp. 987-993, 1997.

- [15] D. Hrovat, D. L. Margolis and M. Hubbard, "An approach towards the optimal semiactive suspension", ASME J. of Dynamic Systems, Measurement and Control, vol. 110, pp. 288-296, September 1988.
- [16] J. K. Hedrick, Hong Keum-Shik and Sohn Hyun-Chul, "Semiactive control of the macpherson suspension system: hardware in the loop simulations", Proc. of the IEEE Conference on Control Applications, vol. 1, pp. 982-987, 2000.
- [17] B. Corbett, "Riding the magnetic wave", Wards Auto World, pp. 49, June 2000.
- [18] Aleksander Hać and Iljoong Youn, "Optimal semiactive suspension with preview based on a quarter car model", Proc. of the 1991 American Control Conference, Green Valley, AZ, vol. 1, pp. 433-438, 1991.
- [19] P. J. Th. Venhovens, "The development and implementation of adaptive semiactive suspension control", Vehicle System Dynamics, vol. 23, pp. 211-235, 1994.
- [20] Alessandro Guida, Carla Seatzu and Giampaolo Usai, "Semiactive suspension design with an optimal gain switching target", Vehicle System Dynamics, vol. 31, no. 4, pp. 213-232, 1999.
- [21] D. Karnopp, M. J. Crosby and R. A. Harwood, "Vibration control using semiactive force generators", ASME J. of Engineering for Industry, vol. 96, no. 2, pp. 619-626, May 1974.
- [22] Mehdi Ahmadian, "A hybrid semiactive control for secondary suspension applications", Proc. of the ASME, Dynamic Systems and Control Division, pp. 743-750, 1997.
- [23] Christopher A. Paré, "Experimental evaluation of semiactive magneto-rheological suspensions for passenger vehicles", Master's Thesis, Mechanical Engineering Department, Virginia Polytechnic Institute and State University, <http://scholar.lib.vt.edu/theses/available/etd-51598-19251/unrestricted/etd.pdf>, May 1998.
- [24] C. Kim and P.I. Ro, "Effect of suspension structure on equivalent suspension parameters", Proc. of the Instn. of Mech. Engrs., Part D, vol. 213, pp. 457-470, 1999.
- [25] A. Stenstrom, C. Asplund and L. Karlsson, "The nonlinear behavior of a macpherson strut wheel suspension", Vehicle System Dynamics, vol. 23, pp. 85-106, 1994.
- [26] T. J. Gordon and M.C. Best, "Dynamic optimization of nonlinear semiactive suspension controllers", International Conference on Control, Part 1, pp. 332-337, 1994.

- [27] Raseem R. Henry and Ashraf A. Zeid, "A nonlinear sub-optimal, observer-based control for semiactive suspension", Transactions of the ASME, Transportation Systems, Dynamic Systems and Control Division, vol. 44, pp. 181-189, 1992.
- [28] I. Ursu, F. Ursu, T. Sireteanu and C. W. Stammers, "Artificial intelligence based synthesis of semiactive suspension systems", Shock and Vibration Digest, vol. 32, no. 1, pp. 3-10, 2000.
- [29] J. C. Smith, Ka C. Cheok and Huang Ningjian, "Optimal parametric control of a semiactive suspension system using neural networks", Proc. of the American Control Conference, vol. 2, pp. 963-967, 1992.
- [30] Ka. C. Cheok and N. J. Huang, "Lyapunov stability analysis for self-learning neural model with application to semiactive suspension system", Proceedings of the IEEE-International Symposium on Intelligent Control, pp. 326-331, 1989.
- [31] Christopher Edwards and Sarah K. Spurgeon, Sliding Mode Control: Theory and Applications, Taylor and Francis, Bristol, PA, ISBN 0-7484-0601-8, 1998.
- [32] C. Kim and P. I. Ro, "A sliding mode controller for vehicle active suspension systems with nonlinearities", Proc. of the Instn. Of Mech. Engrs., Part D, vol. 212, pp. 79-92, 1998.
- [33] Andrew Alleyne and J. K. Hedrick, "Nonlinear adaptive control of active suspensions", IEEE Transactions on Control Systems Technology, vol. 3, no. 1, pp. 94-101, March 1995.
- [34] Makato Yokoyama, J. Karl Hedrick and Shigehiro Toyama, "A model following sliding mode controller for semiactive suspension systems with mr dampers", Proc. of the 2001 American Control Conference, pp. 2652-2657, June 2001.
- [35] E. K. Bender, "Optimal linear preview control with application to vehicle suspension", ASME J. of Basic Engineering, part D, vol. 90, no. 2, pp. 213-221, 1968.
- [36] S.J. Dyke, B.F. Spencer Jr., M.K. Sain and J.D. Carlson, "Modeling and control of magnetorheological dampers for seismic response reduction", Smart Materials and Structures, vol. 5, no. 5, pp. 565-575, 1996.
- [37] C. Richard, M. R. Cutkosky and K. Maclean, "Friction identification for haptic display", Proc. of the 1999 ASME Dynamic Systems and Control Division, v 67, pp. 327-334, 1999.

- [38] Karl J. Åström, “Control of systems with friction”, Proc. of the Fourth International Conference on Motion and Vibration Control, http://www.ifr.mavt.ethz.ch/movic98/proceedings/astrom_knp_c.pdf, 1998.
- [39] Mark R. Jolly, Jonathan W. Bender, and J. David Carlson, “Properties and Applications of Commercial Magnetorheological Fluids”, Proc. of the SPIE 5th Annual Int. Symposium on Smart Structures and Materials, San Diego, CA, March 1998.
- [40] Shawn P. Kelso, Experimental Characterization of Commercially Practical Magnetorheological Fluid Damper Technology”, Proc. of the SPIE Conference on Smart Structures and Materials, Paper No. 4332-34, Newport Beach, CA, March 2001.
- [41] Sekhar Raghavan and J. K. Hedrick, “Observer design for a class of nonlinear systems”, Int. Journal of Control, vol. 59, no. 2, pp. 515-528, 1994.
- [42] J. –J. E. Slotine, J. K. Hedrick, E. A. Misawa, “On sliding observers for nonlinear systems”, ASME J. of Dynamic Systems Measurement and Control, vol. 109, pp. 245-252, 1987.
- [43] E. A. Misawa and J. K. Hedrick, “Nonlinear observers-a state of the survey”, AMSE J. of Dynamic Systems Measurement and Control, vol. 111, pp. 344-352, 1989.
- [44] A.G. Thompson and C. E. M. Pearce, “Physically realizable feedback controls for a fully active preview suspension applied to a half car model”, Vehicle System Dynamics, vol. 30, pp. 17-35, 1998.
- [45] J. J. E. Slotine and W. Li, Applied Nonlinear Control, Prentice Hall, 1991.
- [46] A. Hać, “Adaptive control of vehicle suspensions”, Vehicle System Dynamics, vol. 16, pp. 57-74, 1987.
- [47] William S. Levine, “The Control Handbook”, CRC press, 1996.

FIGURES

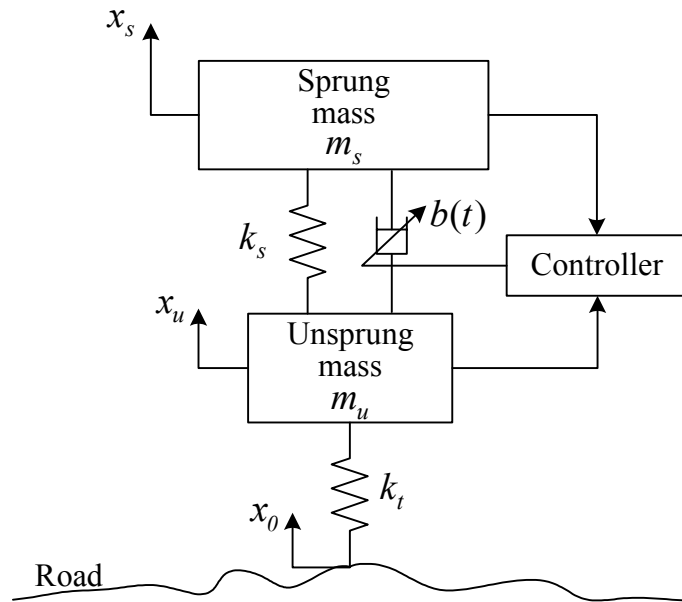


Figure 1: Semiactive quarter-vehicle suspension model

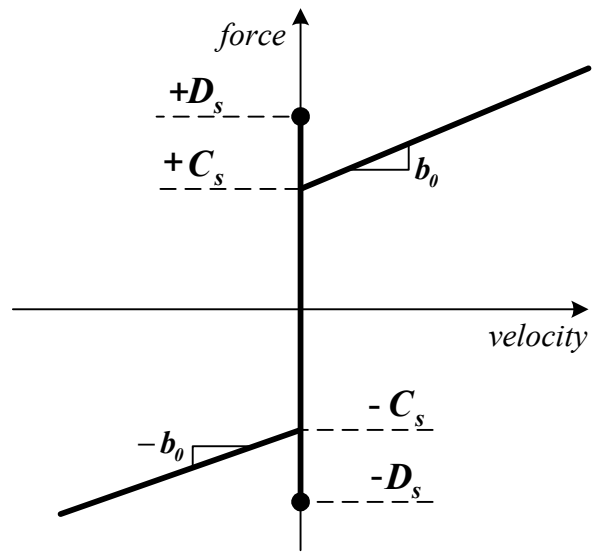


Figure 2: Stiction Model

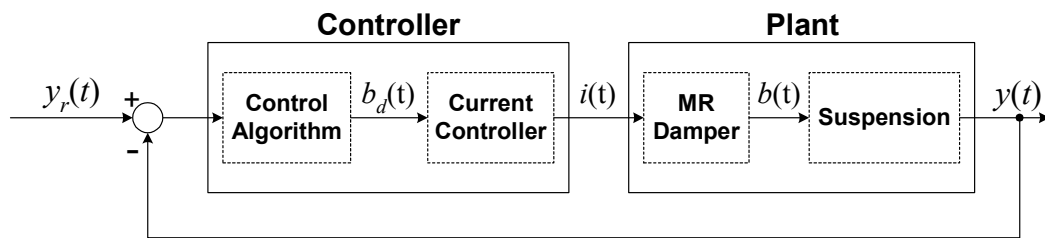


Figure 3: Block diagram of semiactive suspension control system

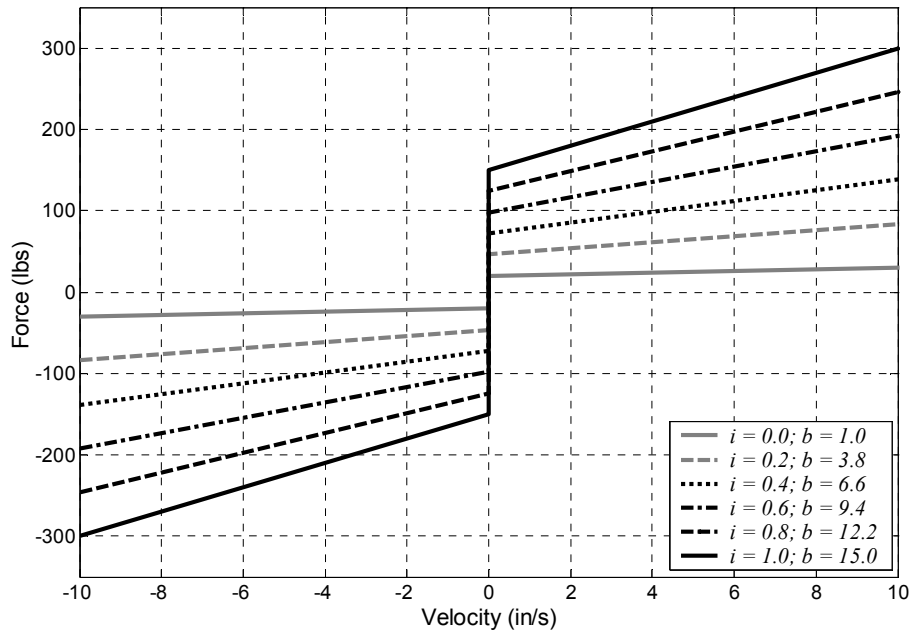


Figure 4: Steady-state damping characteristics of a composite MR damper

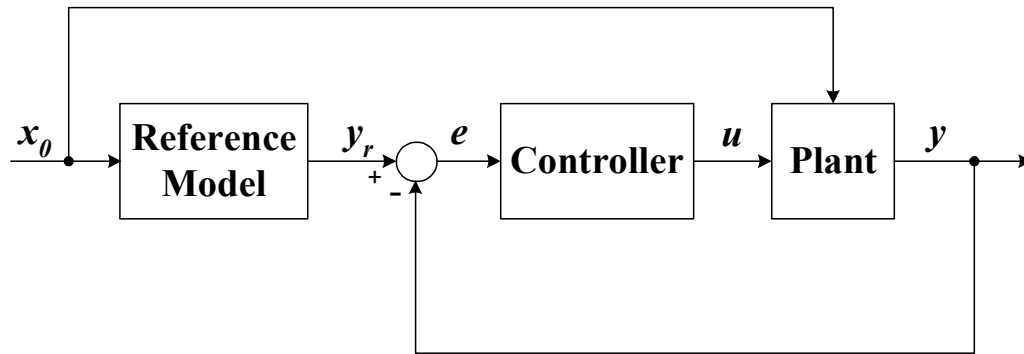


Figure 5: Model Reference Control Structure

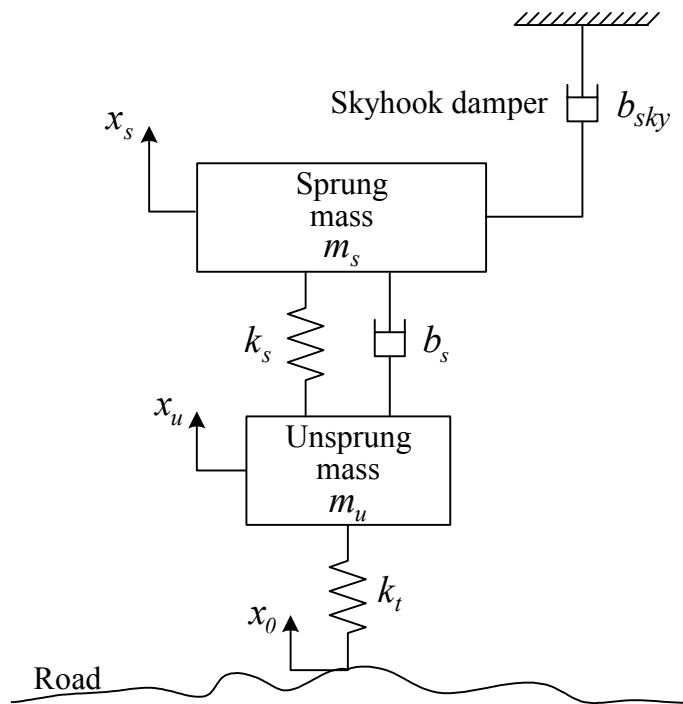


Figure 6: Fourth-Order Skyhook Reference Model

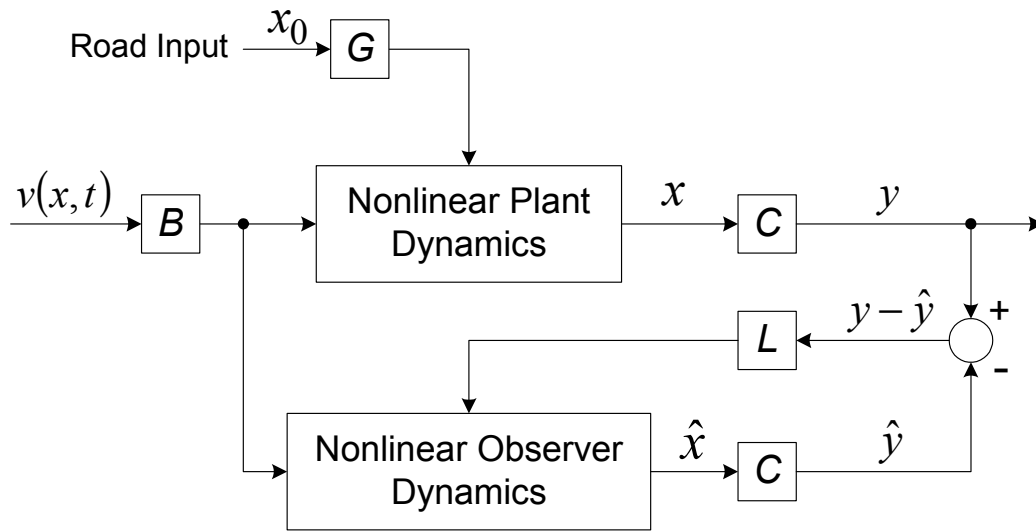


Figure 7: Structure of a conventional nonlinear observer

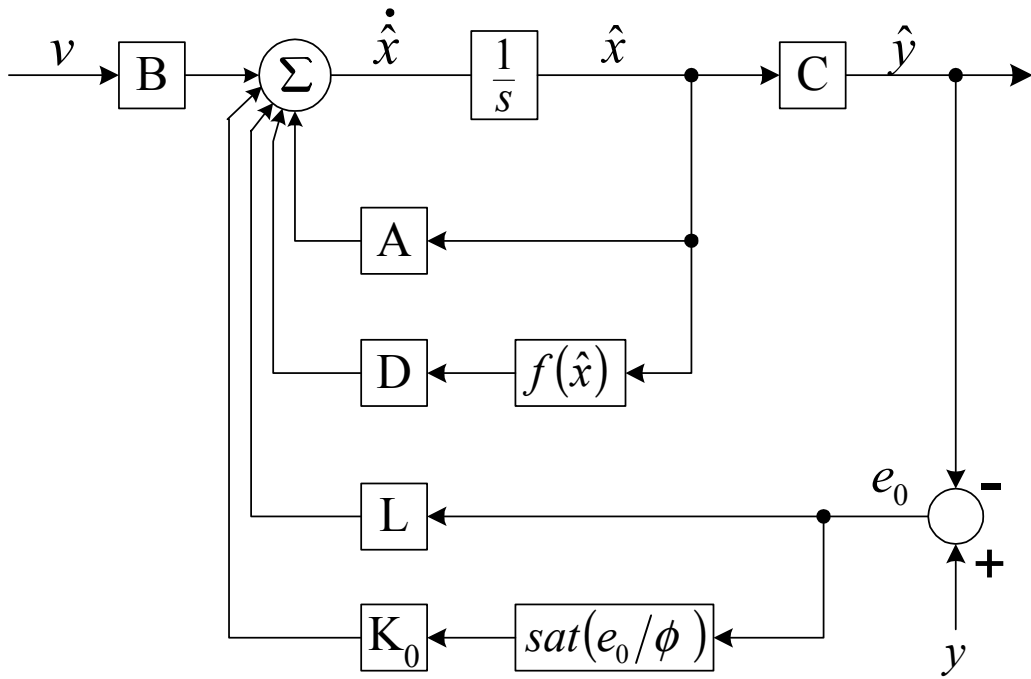


Figure 8: Sliding Mode Observer Structure

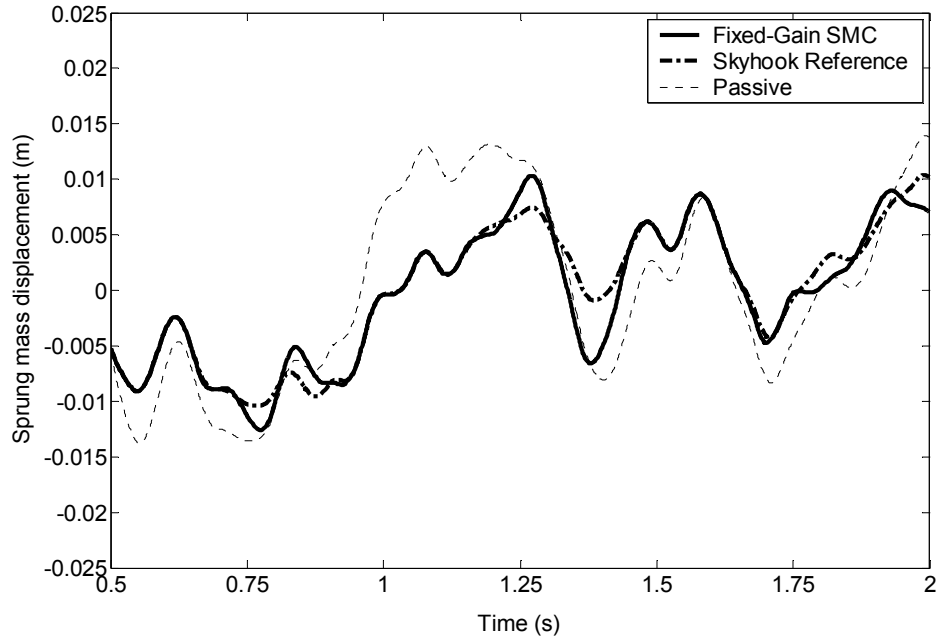


Figure 9: Fixed-gain SMC and nonlinear skyhook reference model responses ($k=10$): low-amplitude white noise road input

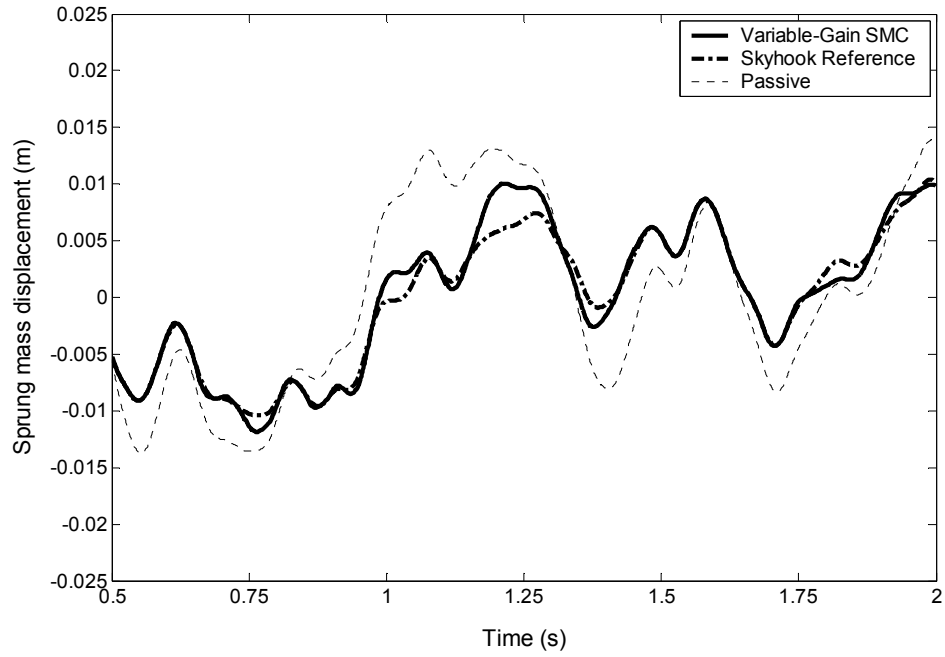


Figure 10: Variable-gain SMC and nonlinear skyhook reference model responses: low-amplitude white noise road input

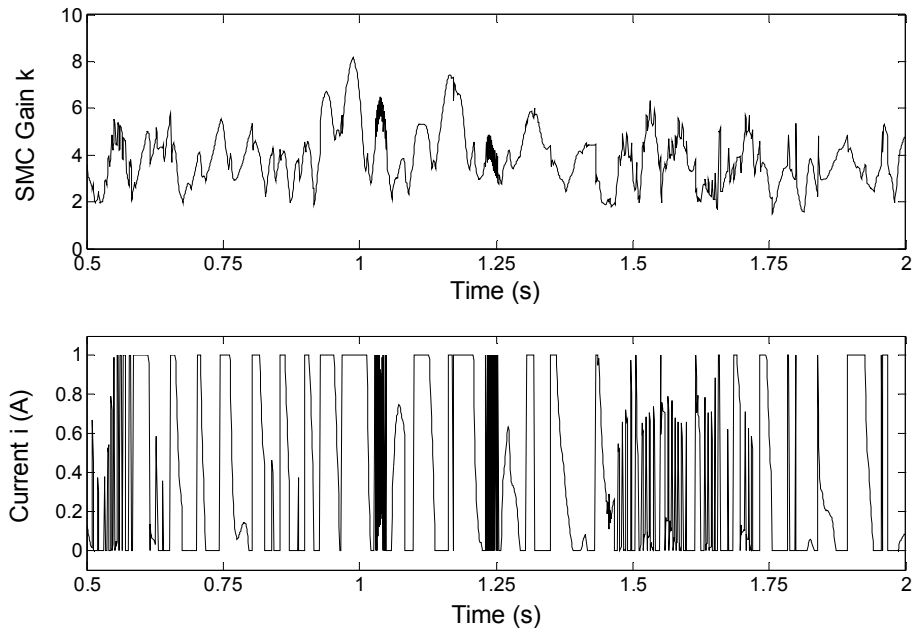


Figure 11: Variable switching gain $k(t)$ and control current $i(t)$ - white noise road input

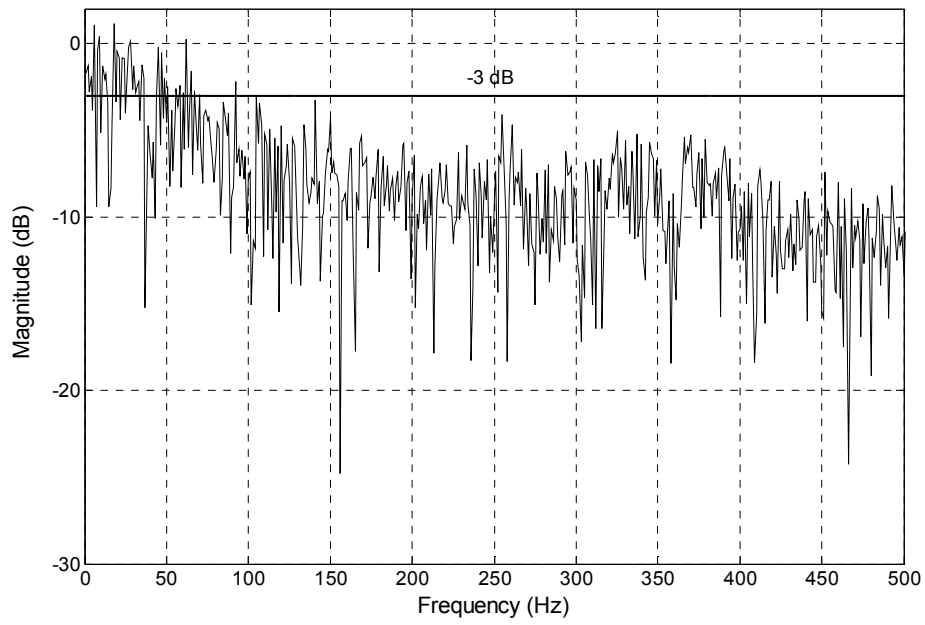


Figure 12: FFT magnitude plot of control current $i(t)$

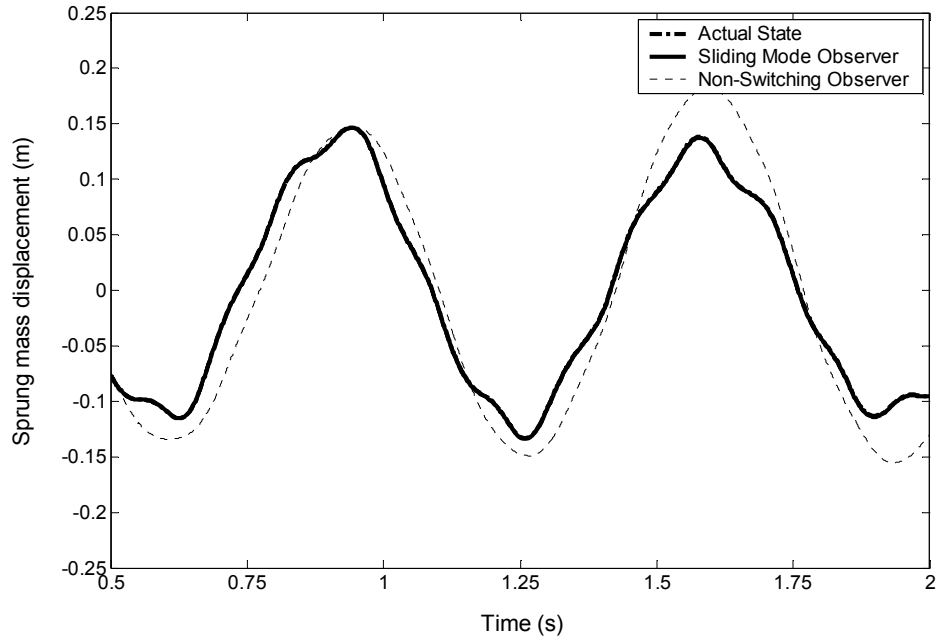


Figure 13: Comparison of SMO, actual, and conventional (non-switching) observer state responses: sinusoidal road input

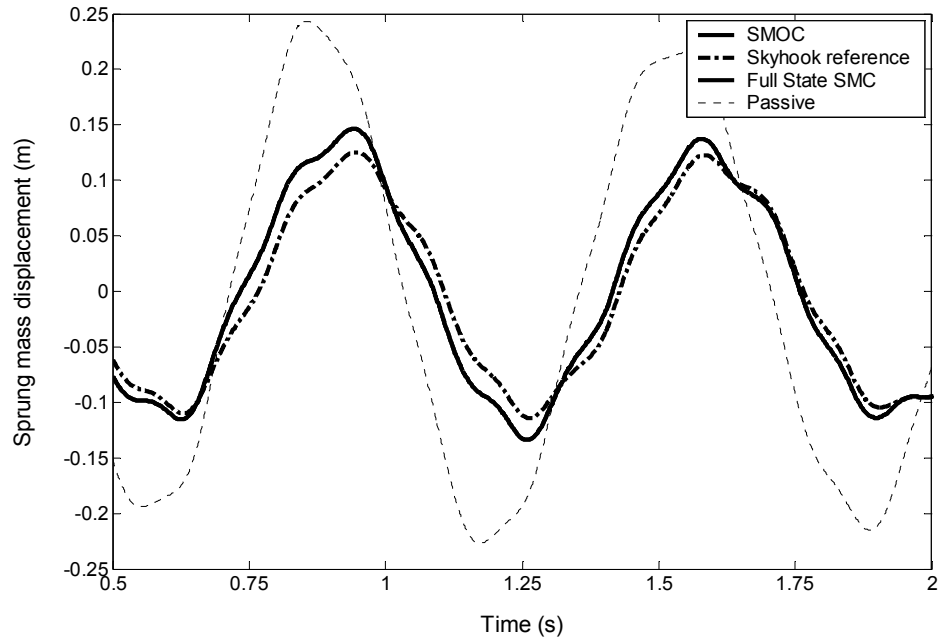
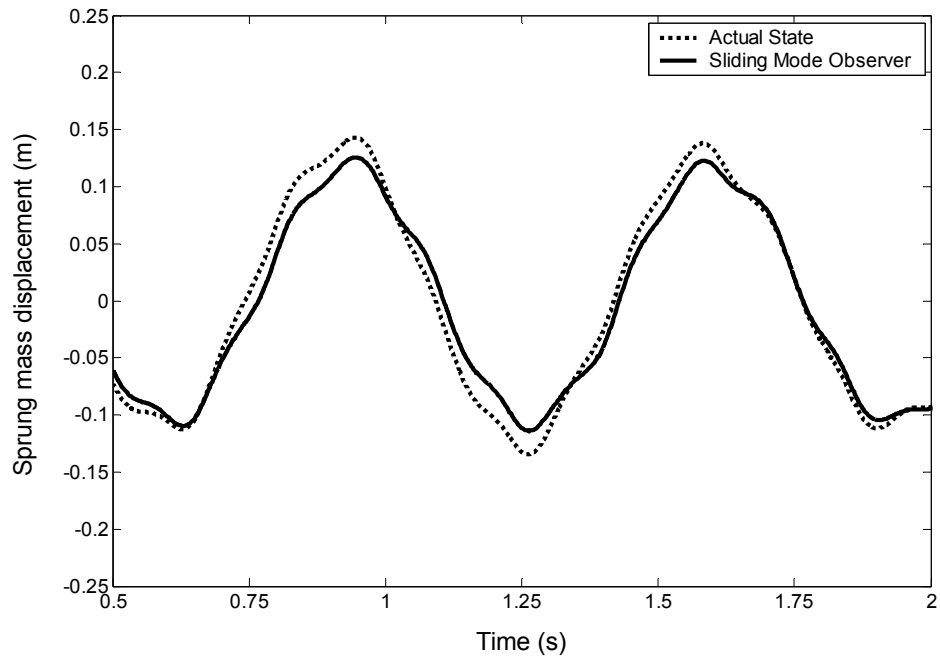


Figure 14: SMOC and skyhook reference responses: sinusoidal road input



**Figure 15: Comparison of actual and SMO state responses with parametric uncertainties:
sinusoidal road input**

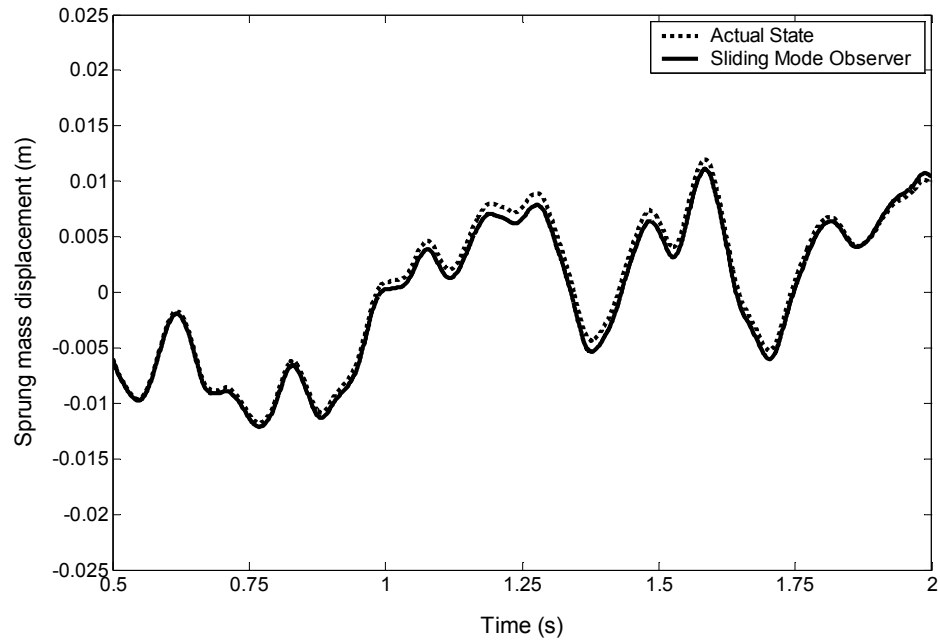


Figure 16: Comparison of actual and SMO state responses with parametric uncertainties: white noise road input

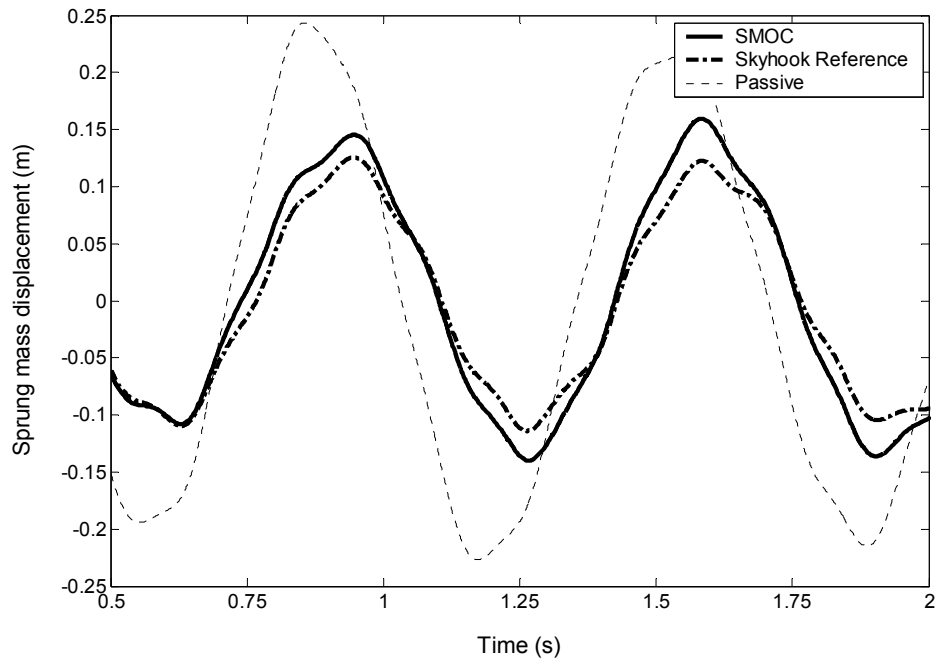


Figure 17: Comparison of skyhook reference and SMOC responses with parametric uncertainties: sinusoidal road input

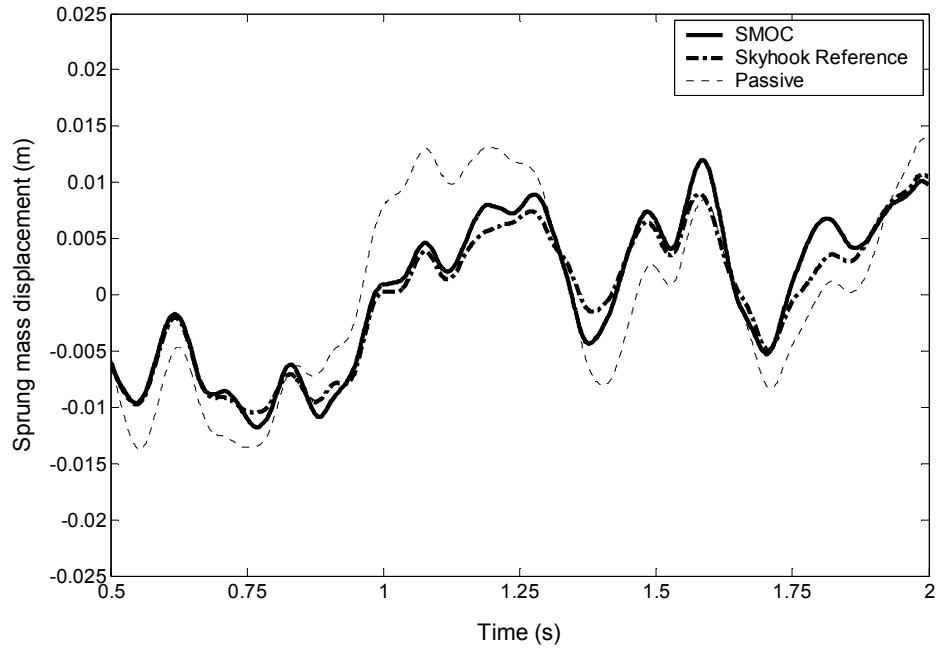


Figure 18: Comparison of skyhook reference and SMOC responses with parametric uncertainties: white noise road input

TABLES

Table 1: Simulation Summary

	Simulation Set	Objective
I	Fixed-Gain vs. Variable-Gain SMC	Evaluate implications of fixed and variable gain switching on SMC performance
II	Sliding Mode Observation and Control (SMOC)	Evaluate the performance of sliding mode observation and control (SMOC)
III	SMOC with Parametric Uncertainties	Investigate the impacts of parametric uncertainties on SMOC

Table 2: Nonlinear vehicle suspension parameters

Parameter	Description	Value
m_s	Sprung mass	240 kg
k_{s1}	Linear suspension stiffness	12394 N/m
k_{s2}	Nonlinear suspension stiffness	-73696 N/m ²
k_{s3}	Nonlinear suspension stiffness	3170400 N/m ³
m_u	Unsprung mass	25 kg
k_t	Tire stiffness	160000 N/m
b_0	Nominal suspension damping	193 Ns/m
$b_p = b_s$	Passive system damping	1385.4 Ns/m
b_{\max}	Maximum system damping	2633 Ns/m

Table 3: Comparison of fixed and variable gain SMC for white noise road input

	Passive Damping	Skyhook Reference	Fixed-Gain SMC	Variable-Gain SMC
Performance Index J_1	3.92	0	0.89	0.70
Performance Index J_2	9.49	0	5.84	3.99
Performance Index J_3	55.15	45.51	68.99	59.16
Peak Suspension Travel (cm)	5.38	5.89	6.96	6.84
Peak Sprung Mass Acceleration (m/s/s)	9.88	8.99	14.41	12.24

Table 4: Comparison of SMO and conventional (non-switching) observers: sinusoidal road input

Observer strategy	J_4	J_5
SMO	0.44	0.81
Conventional	25.04	67.60

Table 5: Comparison of SMOC and full-state SMC performance: sinusoidal road input

	Passive Damping	Skyhook Reference	Full-State SMC	SMOC
Performance Index J_1	92.39	0	16.09	16.30
Performance Index J_2	165.47	0	39.47	39.71
Performance Index J_3	2106.67	1400.32	1690.50	1698.89
Peak Suspension Travel (cm)	28.62	25.44	27.75	27.69
Peak Sprung Mass Acceleration (m/s/s)	55.40	36.52	50.87	50.21

Table 6: SMOC performance with parametric uncertainties: sinusoidal road input

	Passive Damping	Skyhook Reference	SMOC
Performance Index J_1	90.52	0	16.31
Performance Index J_2	162.52	0	37.92
Performance Index J_3	1706.23	993.83	1185.65
Peak Suspension Travel (cm)	28.38	24.23	26.22
Peak Sprung Mass Acceleration (m/s/s)	54.88	36.67	44.32

Table 7: SMOC performance with parametric uncertainties: white noise road input

	Passive Damping	Skyhook Reference	SMOC
Performance Index J_1	3.79	0	1.03
Performance Index J_2	9.21	0	3.91
Performance Index J_3	55.15	49.70	63.93
Peak Suspension Travel (cm)	5.38	5.86	6.75
Peak Sprung Mass Acceleration (m/s/s)	9.88	9.97	13.63